Using a Level-Set model to estimate dwell time in a vacuum dewatering process for paper

K. Rezk*, Jan Forsberg, Lars Nilsson and Jonas Berghel
Department of Energy-, Environmental and Building Technology, Karlstad University
*Corresponding author: SE-651 88 Karlstad, Kamal.Rezk@kau.se

Abstract: A numerical model of a paper sheet was created using a Level-Set method to analyse a vacuum dewatering process. A 2D representation of the paper model was created in Matlab with randomly positioned circular fibres and identical orientation in one dimension. The model considers the influence of the forming fabric which the paper sheet is placed on during the vacuum process. The forming fabric was modelled using volume forces to represent flow resistance in the momentum equation.

The coupled LS method was used to estimate dry content of fibres during various dwell times for fifteen different structures. The correlation between dry content and dwell time was compared for each structure. Random positioning of the fibres impacts the dwell time slightly depending on the amount of narrow regions. Future studies include analysis of random orientation of the fibres as well as deformation and displacement of fibres during the dewatering process.

Keywords: CFD, Two-Phase flow, Level-Set method, Navier-Stokes, Vacuum dewatering

1. Introduction

Water removal during pulp manufacturing is an intensive energy use process. The dewatering process generally consists of four stages in which the first stage, water is removed due to gravity and low vacuum filtration. In the second stage, a higher level of vacuum is applied though a suction box. During this section, most of the water in the fibre suspension is removed. The third stage of drying is performed in the press section by compressing the paper fabric in which the fibre network is collapsed. During the press section, water is mechanically removed from the fibre web. The final stage consists of thermal drying in which the remaining water is evaporated on steam-heated cylinders.

Extensive experimental studies on mechanical dewatering processes have been conducted throughout the years. Åslund and Vamhoff [1] [2] have developed methods for studying mechanisms during a one suction pulse such as web compression, displacement of water by air and rewetting. They concluded through their work that web deformation is the dominant dewatering mechanism and addressed the issue of rewetting and how to minimize its effect. Roux and Rueff [3] developed a drainage model which states that at a constant suction pressure, the amount of filtrate per unit surface area is proportional to the square root of the suction time.

A review of existing literature presents no extensive research of numerical studies of two-phase flow applied on vacuum dewatering processes on paper sheets. However, numerous researchers have studied flow mechanics in paper models such as Zhu et al. [4], Nilsson and Stenström [5] [6], Jackson and James [7]. Their studies involve analysis of singles-phase flow in different arrangements of fibre networks in which both creeping and non-creeping flow has been studied.

In this study, a 2D model of the paper sheet is analysed numerically using a Level-Set (LS) method. The model of the paper sheet is composed of cylindrical fibres with a diameter and bound water content typical of kraft softwood. The geometrical shape and positioning of the fibres are created in a Matlab-code and imported to Comsol. The purpose of analysing vacuum dewatering numerically is to gain a physical understanding of the process. The aim is to estimate the dwell time for fifteen different structures. The models to be compared have a basis weight of 20 g/m^2 and a porosity of 0.72. The fibre walls are not considered in the model as we assume no deformation and constant saturated level of water.

2. Governing Equations

As water is removed from the paper sheet, air penetrates the pores of the paper. In order to consider two different phases of fluids in the same system, the LS method is applied. The LS method is a numerical technique for tracking interfaces and shapes. The LS function is used to locate fluid-fluid interface in which the function takes a positive or

negative value depending on which side of the interface is viewed.

$$\varphi(\vec{x},t)=\begin{cases}>0\ if\ \ \vec{x}\ \in\ water\\ =0\ if\ \ \vec{x}\ \partial\Omega\\ <0\ if\ \ \vec{x}\ \in air\end{cases} \quad (1)$$

where $\varphi(\vec{x},t)$ is the LS function and $\partial\Omega$ is the interface boundary. The mechanisms for the interface movement are defined with an Eulerian formulation

$$\frac{\partial\varphi}{\partial t}+u_j\frac{\partial\varphi}{\partial x_j}=0 \quad (2)$$

where the first term in this PDE is the local time derivative of the LS function and the second term is the transportation of the function through advection. The LS function is defined as a signed distance function for which $\varphi(\vec{x})=0$ when $\vec{x}$ is on the interface boundary $\partial\Omega$. The signed distance function is approximated numerically in order to achieve smoothness of the solution. This is achieved with a first-order accurate smeared-out approximation using a Heaviside function.

As Eq. (2) is solved during a simulation process, the movement of the fluid-fluid interface changes the LS function which causes the smeared interface thickness to vary. Achieving a constant interface thickness minimizes numerical error due to smearing. Consequently, Eq. (2) is extended with a re-initialisation term

$$\frac{\partial\varphi}{\partial t}+u_j\frac{\partial\varphi}{\partial x_j}=\gamma\frac{\partial\varphi}{\partial x_j}\left(\varepsilon\frac{\partial\varphi}{\partial x_j}-\varphi(1-\varphi)\frac{\partial\varphi}{\partial x_j}\left|\frac{\partial\varphi}{\partial x_j}\right|^{-1}\right) \quad (3)$$

where γ is the re-initialisation parameter. Both the density and viscosity is a function of the LS function in order to achieve a smooth transition in material properties over the interface.

In the two-phase system, the governing equations for mass and momentum is calculated. A direct numerical simulation with the Navier-Stokes (NS) equations was implemented in the CFD software, COMSOL MultiPhysics 4.2a.

$$\frac{\partial u_i}{\partial x_i}=0 \quad (4)$$

$$\rho u_j\frac{\partial u_i}{\partial x_j}=-\frac{\partial p}{\partial x_i}+\mu\left[\frac{\partial}{\partial x_j}\left(\frac{\partial u_i}{\partial x_j}+\frac{\partial u_j}{\partial x_i}\right)\right]-\rho g_i+F_i+F_{st,i} \quad (5)$$

Notice from Eq. (5) that the two last terms represent sources in the NS equations. The first term is a momentum source term which represents the flow resistance exerted by the forming fabric. The last source represents surface tension on the fibre walls.

3. Computational domain

The 2D-model of the paper sheet is composed of cylindrical fibres with a diameter and bound water content typical of kraft softwood fibres. A Matlab-code was developed to create fibres and randomly position them throughout the domain which represents the paper. The code was set to create an amount of fibres comprising a basis weight of 20 g/m^2 and a porosity of approximately 0,72. Fifteen different structures were created in Matlab. The paper is pressed on a forming fabric during the vacuum pulse. The influence of the fabric on the flow process is described with volume forces. Displacement and deformation of the fabric geometry over time are disregarded in these simulations. Moreover, the orientation of each fibre is in 1-dimension which is a requirement for 2D simulations, see Fig. (1).

The dewatering process occurs under high vacuum pressures which causes large velocity gradients as the space of the dimension in the computational domain is of the order of 10e^{-5} m. As air is gradually filling the pores of the domain, local Re numbers are rapidly increasing. Even though the Re number is relatively low, large velocity gradients occur at the curvature of the fibre walls at narrow regions. The advective terms in Eq. (5) will therefore cause disturbances in the solution as they vary significantly. In order to minimize these disturbances, an artificial diffusion parameter is applied to the NS equations which will smooth out the disturbances.

3.1 Initial and boundary conditions

Initially, the 2D representation of the paper and the forming fabric is contained with water. The diameter of the fibre considers a saturated state of water. During the vacuum process, the bound water is presumed of not separating from the fibre wall as we disregard

deformation. The grey zone in Fig. (1) is air and the blue zone represents water. The boundary that connects these zones is the initial LS interface.

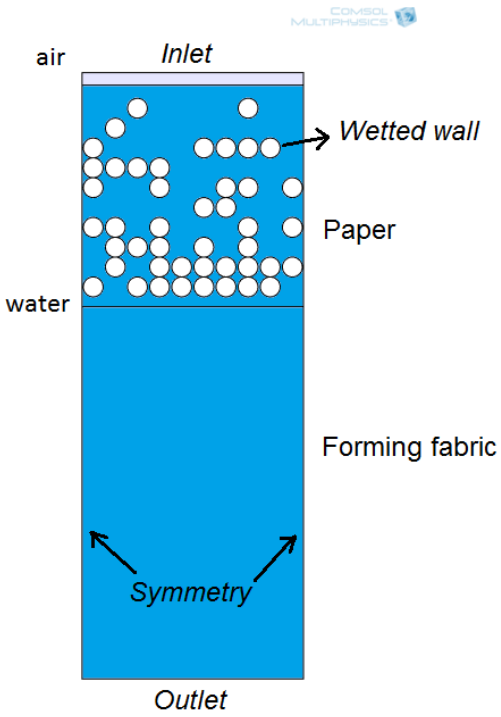

Fig. (1). A 2D representation of the paper sheet at the top of a forming fabric

The boundary conditions for the 2D-model in Fig. (1) are

- *Pressure, no viscous stress*
- *Symmetry*
- *Wetted wall*

Pressure was applied at the inlet and outlet boundary in which the vacuum level was set at 40 kPa at the outlet and reference pressure at 0 Pa was set at the inlet. Symmetry was set at the vertical boundaries as the fibre structure of the domain which was considered characteristic. The wetted wall function was applied at the fibre walls as it provides more numerical stability than the no-slip conditions. The equation indicates a slip condition at the fibre walls. In addition, the condition adds a frictional force which is dependant of the local mesh size at the wall.

The simulation model is solved transient where the CFD program chooses appropriate time steps depending the relative numerical error. A stop criterion was implemented to inform the solver to end the simulation if the volume fraction of the suspended water reaches a level 0.01.

3.2 Model implementation

The yarns that comprise the forming fabric are not modelled as we include volume forces. Rough calculations of the characteristic Reynolds (Re) number indicate influence of inertial forces. Hence, considering Darcy's law alone to volume average the flow will underestimate flow resistance. Instead, Forchheimer's equation is used to characterize flow resistance

$$F_i = \alpha_{V_{ij}} u_j + \alpha_{I_{ij}} u_j |u_j| \qquad (6)$$

where F_i and u_j are vectors that denote the volume force (N/m^3) and velocity field (m/s), respectively. The $\alpha_{V_{ij}}$ and $\alpha_{I_{ij}}$ coefficients represent viscous and inertial resistance respectively. The viscous resistance coefficient represents energy losses due to viscous forces at the air-water/fibre wall interface. The inertial resistance coefficient is related to the geometric properties of the porous medium, as it is related to inertial forces. The resistance coefficients in Eq. (6) are determined by the geometric structure of the forming fabric and the boundary layer development. The viscous and inertial terms are viewed as coefficient matrices. They are implemented in the porous model as constant domain properties, in which, they act as flow resistance coefficients and are dependant of direction of the flow velocity.

A 3-dimensional flow representative volume (FRV) was created for the yarn structure with a yarn diameter of 0.16 mm and a hydraulic diameter of 0.2 mm. Single phase simulations of air and water were simulated in the FRV-model in which a force and momentum flow balance was set up

$$\sum F_{loss} = \int_{A_{out}} p_{out}\, dA + \rho \int_{A_{out}} u_{out}^2 dA - \int_{A_{in}} p_{in} dA - \rho \int_{A_{in}} u_{in}^2 dA \qquad (7)$$

where the term on the left hand side of Eq. (7) is the sum of momentum losses and pressure acting on the flux boundaries. The volume force acting on the flow of the forming fabric is determined by dividing Eq. (8) with the volume of the fluid domain so that the forces are inflicted over a volume unit,

$$\langle F_i \rangle = \frac{\sum F_{loss}}{V_{FRV}} \qquad (8)$$

moreover, the velocity in the FRV-model is volume averaged according to

$$\langle u \rangle_{FRV} = \frac{1}{V_{FRV}} \int_{V_{FRV}} u \, dV \qquad (9)$$

Eq. (6) is rewritten with volume averaged coefficients from Eq. (8) and Eq. (9).

$$\langle F_i \rangle = \alpha_{V_{ij}} \langle u_j \rangle_{FRV} + \alpha_{I_{ij}} \langle u_j \rangle_{FRV} \langle |u_j| \rangle_{FRV} \qquad (10)$$

Twelve velocity-force (u-F) correlations were established from the FRV-model for each phase. In Eq. (10), the resistance coefficients require a solution. The least square method was applied in a MATLAB code in order to achieve an approximate solution on these coefficients. Importing a series of velocity vectors $\langle u_j \rangle_{FRV}$ and $\langle u_j \rangle_{FRV} \langle |u_j| \rangle_{FRV}$, and the volume force vector $\langle F_i \rangle$ into MATLAB yields four coefficients for each phase.

Implementing these coefficients in the paper model in Fig. (1), the LS function is used to distribute the value of the coefficients for each phase and over the interface thickness.

$$\begin{cases} \alpha_{V,yx} = \alpha_{V,water} \varphi + \alpha_{V,air} (1 - \varphi) \\ \alpha_{V,yy} = \alpha_{V,water} \varphi + \alpha_{V,air} (1 - \varphi) \end{cases} \qquad (11)$$

$$\begin{cases} \alpha_{I,yx} = \alpha_{I,water} \varphi + \alpha_{I,air} (1 - \varphi) \\ \alpha_{I,yx} = \alpha_{I,water} \varphi + \alpha_{I,air} (1 - \varphi) \end{cases} \qquad (12)$$

The volume force sink term is implemented in the lower water domain of Fig. (1) as

$$F_y = \left(\alpha_{V_{yx}} u_x + \alpha_{V_{yy}} u_y \right) \frac{1}{\varepsilon_p} + \left(\alpha_{I_{yx}} u_x + \alpha_{I_{yy}} u_y \right) \frac{|u_j|}{{\varepsilon_p}^2} \qquad (13)$$

where ε_p is the porosity of the forming fabric. The porosity is used to scale the velocities in the volume force domain so they are correlated to the velocities in the FRV-model.

3.3 Mesh grid

An unstructured mesh grid containing triangle elements was created for the paper models, see Fig. (2). The grid is solved in a finite element space where a set of basis functions are used to create piecewise linear relations between the mesh elements and convert them to weak formulations for them to be solved. A direct linear system solver was used coupled with a time-dependant second order BDF solver. The direct solver is called PARDISO which handles sparse linear systems using LU factorization to compute a solution. More information on the solver is found in COMSOL documentation. The BDF solver performs time stepping using a backward differentiation with a maximum order of accuracy of 2, which is the degree of the interpolating polynomial.

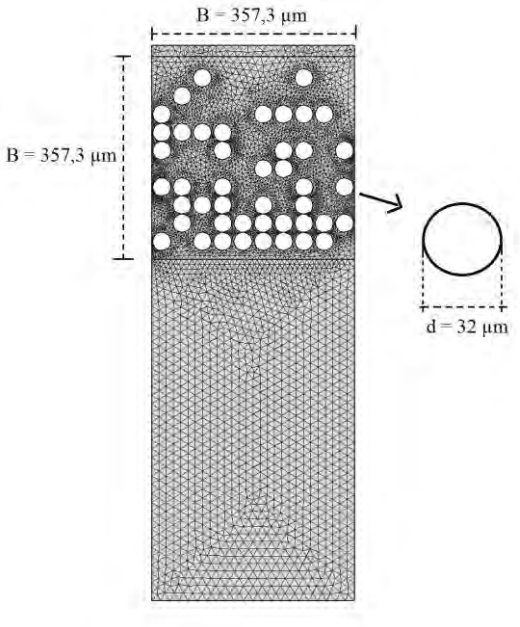

Fig. (2). Grid resolution of a paper model on top of a forming fabric

The same mesh grid resolution was used for all 20 g/m^2 models (standard case) wherein the maximum mesh element size was set to 16,5 µm, the minimum element size were 7,15 µm, the resolution of narrow regions was set to 1 and the element growth rate was set to 1,15. The sensitivity of the grid was tested by varying these element specifications for eight cases on structure_7, see Table (1).

Table (1). Grid element parameters

	Max. ele. size	Min. ele. size	Ele. growth rate	Res. of narrow reg.
Case 1	**12,5 µm**	7,15 µm	1,15	1
Case 2	**10,0 µm**	7,15 µm	1,15	1
Case 3	16,5 µm	**3,57 µm**	1,15	1

Case 4	16,5 µm	**1,43 µm**	1,15	1
Case 5	16,5 µm	7,15 µm	**1,05**	1
Case 6	16,5 µm	7,15 µm	**1,025**	1
Case 7	16,5 µm	7,15 µm	1,15	**3**
Case 8	16,5 µm	7,15 µm	1,15	**5**

The difference in dwell time and simulation time is presented for a model with a basis weight of 20 g/m^2 in Table (2).

Table. (2). Comparison of dwell time and simulation time for different grid structures

	Dwell time [ms]	Simulation time [s]	Number of grid points
Case standard	0,544	4420	10104
Case 1	0,647	6651	11215
Case 2	0,650	9887	13172
Case 3	0,559	8481	15979
Case 4	0,559	8481	15979
Case 5	0,648	7923	18000
Case 6	0,623	13529	26987
Case 7	0,704	9094	15012
Case 8	0,788	16084	23352

It is viewed in Table (2) that the dwell time increases as the mesh structure becomes denser. The movement of the interface is determined by the number grid points in which numerical interpolation is used to estimate the location of φ. The exact location of φ could hypothetically be determined with an infinite number of grid points. In this case, however, the dwell time is underestimated with coarser structures.

4. Numerical trial

Fifteen simulations were conducted on paper models with basis weight of 20 g/m^2 and a porosity of approximately 0.72. These models were compared with each other in order to investigate the significance of the positioning of fibres. Dewatering rate, dry solids content and dwell time were correlated between the models. Values of dewatering rate and dry solids content were registered for every time step in the transient solver and imported to Matlab for further analysis.

5. Results and discussion

The dwell times for all fifteen simulations are presented in Table (3).

Table. (3). Comparison of dwell time for all structures

	Dwell time [ms]
Structure_1	0,478
Structure_2	0,496
Structure_3	0,926
Structure_4	0,809
Structure_5	0,481
Structure_6	0,999
Structure_7	0,544
Structure_8	0,456
Structure_9	0,437
Structure_10	0,572
Structure_11	0,555
Structure_12	0,492
Structure_13	0,465
Structure_14	0,506
Structure_15	0,396

Viewing the results, it shows a wide variation on the dwell time. However, the dewatering rate is vastly reduced at the end of all simulations. Due to minor fluctuations on the dewatering rate, it could result in large differences in dwell time as an exact value of the dry solids content is used as the stop criterion.

The rate of change of solid dry content over time is compared for three selected models, see Fig. (3). At the start of each process, the dewatering rate is low as water is accelerated from a standstill. The dewatering rate differs with time due to random fibre arrangement, see Fig. (4). Due to the fact of fluctuating dewatering rates, the maximum dry solid content is reached for different dwell times. However, the difference in dry solids content is minor at a time of 0.5 ms according to Fig. (3).

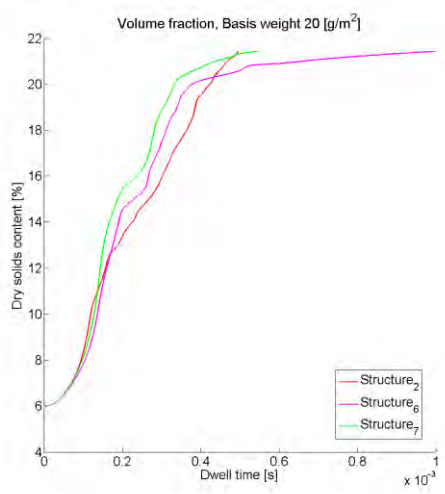

Fig. (3). Correlation between solid dry content and dwell time for four different 20 g/m^2 models

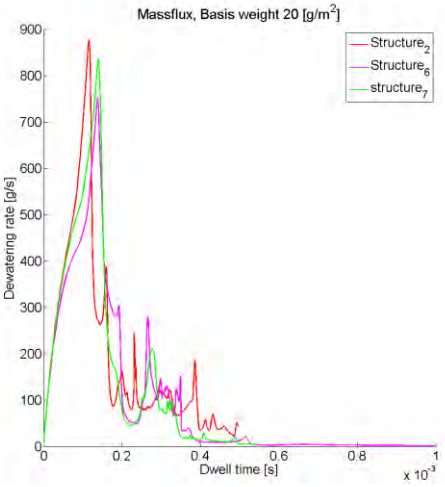

Fig. (4). Correlation between solid dry content and dwell time for four different 20 g/m^2 models

This indicates that random fibre positioning has a minor effect on the dwell time during high vacuum levels. Lower values on the vacuum pulse could result in different outcomes. The factors that dictate the result are, as expected, basis weight and porosity. The influence of the forming fabric is minor as fibre diameter is a factor five higher and also has a coarser arrangement than the paper sheet.

The influence of the isotropic diffusion term was verified as five different values in the range of 0,2 – 0,4 was tested on a 20 g/m^2 model. It shows that the dwell time differs approximately 1-2% between these values. The effect of the isotropic diffusion coefficient is insignificant due to low Re numbers during a long stretch of the dewatering process. As the volume of air is continuously growing in the paper model, the velocity magnitude and gradients increase rapidly. During these conditions, disturbance in the model occur in which the isotropic diffusion coefficient dampens the solution. Hence, lower values than 0,2 could not be achieved as the solution becomes unstable at the end of the dewatering process.

The volume fraction and the dewatering rate is presented for all cases in the mesh sensitivity study, see Fig. (5-6). The figures indicate no major variation on the volume fraction. In Fig. (6) the dewatering rate starts to fluctuate as the water content in the pore space is emptied. These fluctuations deviate for different mesh cases. The determination of the dwell time is dominated by the amount of narrow regions in which water is retained by capillary forces close to the fibre walls.

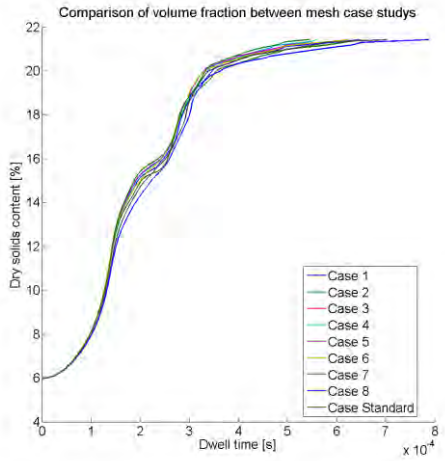

Fig. (5). Comparison of dry solids content for all mesh cases

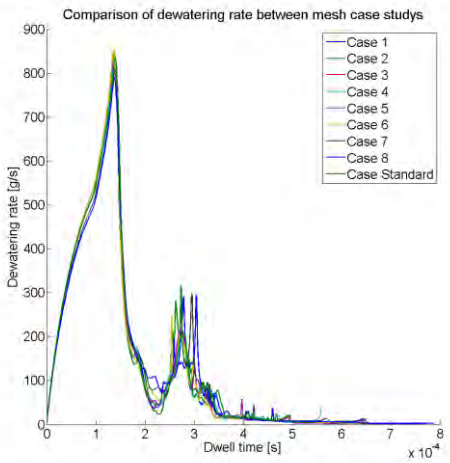

Fig. (6). Comparison of dewatering rate for all mesh cases

In our first approach to establish a numerical model of a vacuum dewatering process, we have excluded the influence of web deformation. Based on the studies of Åslund and Vamhoff [1] [2], they state that web deformation plays an important role in the dewatering rate. Test simulations have been conducted on models with basis weight of 20 g/m^2 with elliptical fibre forms randomly positioned. It had negligible effects on the dwell time. However as the fibre is continuously deforming, water is removed from the wall which is not considered in the model. As deforming is not considered in the model, expansion of the fibres are disregarded which excludes the influence of rewetting which was also stated as an important dewatering factor by Åslund and Vamhoff.

Due to high vacuum levels and as water is removed, the fibres should collapse on top of each other, forming a compact bed of fibres. This should decrease the permeability of the paper sheet model which would result in longer dwell times. The influence of deformation and fibre displacement could be analysed numerically by implementing an Arbitrary Lagrange-Eulerian (ALE) method which handles moving mesh. Based on previous literature, these parameters ought to be analysed and implemented in future models.

The arrangement of fibres in experimental data has random orientation. This could not be considered in the numerical models due to 2D representation. In order to analyse the influence of random orientation, a LS 3D-model is a possible approach which would require a large amount of data resources. Implementation of volume forces is an additional method for which random orientation is considered. The approach is based on creating a flow representative volume of random fibre orientation in a 3D-environment and conducting single-phase flow simulations of water and air in order to create volume forces. The dynamic of the dewatering rate will be lost which will make it difficult to put it into correlation. However, a more accurate numerical model could be established in terms of achieving a valid dwell time.

6. Conclusion

A numerical model of a vacuum dewatering process was established as the LS method was applied to simulate two-phase flow phenomena in a 2D paper sheet model. Models with basis weights of 20 g/m^2 and porosity of 0.72 were simulated wherein fifteen 20 g/m^2 models were used to analyse the influence of random positioning of fibres. The result shows minor influences of different structures on the dewatering process. The mesh case study indicates low sensitivity of the models which support their validity.

Future studies include consideration of fibre deformation and displacement during a vacuum dewatering process. Moreover, random fibre orientation will be studied by using volume forces to represent flow resistance.

7. References

[1] Åslund, P & Vomhoff, H. Method for studying the deformation of a fibre web during a suction pulse. *Nordic pulp & paper research journal,* 23 (4), 398-402. (2008)

[2] Åslund, P., Vomhoff, H. & Waljanson, A. The deformation of chemical and mechanical pulp webs during suction box dewatering. *Nordic pulp & paper research journal,* 23 (4), 403-408. (2008)

[3] Roux, J. & Rueff, M. Characterization of the fiber–water separation process through a suction box of a single-wire pilot paper machine. *Separation and Purification Technology,* 92 (0), 136-142. (2012)

[4] Zhu, S., Pelton, R.H. & Collver, K. Mechanistic modelling of fluid permeation through compressible fiber beds. *Chemical Engineering Science,* 50 (22), 3557-3572. (1995)

[5] Nilsson, L. & Stenström, S. Effects of serial and parallel pore non-uniformities: Results from two models of the porous structure. *Transport in Porous Media,* 25 (3), 335-350. (1996)

[6] Nilsson, L. & Stenström, S. A study of the permeability of pulp and paper. *International Journal of Multiphase Flow,* 23 (1), 131-153. (1997)

[7] Jackson, G.W. & James, D.F. The permeability of fibrous porous media. *The Canadian Journal of Chemical Engineering,* 64 (3), 364-374. (1986)